

## Article

# Aging of Limestones and Silane–Siloxane-Based Protective Hydrophobics: The Impact of Heating–Cooling and Freeze–Thaw Cycles

Carla Lisci <sup>1,2</sup> , Fabio Sitzia <sup>1,2</sup> , Vera Pires <sup>1,3</sup>  and José Mirão <sup>1,2,\*</sup> 

<sup>1</sup> HERCULES Laboratory and IN2PAST, Associate Laboratory for Research and Innovation in Heritage, Arts, Sustainability and Territory, Institute for Advanced Studies and Research, University of Évora, Largo Marquês de Marialva 8, 7000-809 Évora, Portugal; clisci@uevora.pt (C.L.); fsitzia@uevora.pt (F.S.); vlcpi@uevora.pt (V.P.)

<sup>2</sup> Geosciences Department, School of Sciences and Technology, University of Évora, Rua Romão Ramalho 59, 7000-671 Évora, Portugal

<sup>3</sup> LEM Laboratório de Ensaios Mecânicos da Universidade de Évora, Rua Romão Ramalho 59, 7000-671 Évora, Portugal

\* Correspondence: jmirao@uevora.pt

**Abstract:** Stones are traditionally used in construction and architectural applications as building elements due to their aesthetic and technical/structural performance. Like other environmental factors (rain, humidity, moisture, salt presence, biological activity, etc.), heating–cooling and freeze–thaw cycles significantly threaten the longevity of stone materials. Hence, considering the socio-economic and cultural value of stones, preventive actions such as hydrophobic coatings are applied to prevent or mitigate damage. The scope of this study is the performance assessment of limestones with different characteristics and the efficiency of various commercial silane/siloxane-based hydrophobic coatings when exposed to thermal variation and freeze–thaw. For that purpose, the standards EN 14066:2013 (determination of resistance to aging by thermal shock) and EN 12371:2010 (determination of frost resistance) were followed. Open porosity and static contact angles were estimated to assess the stone durability and water protection capabilities of the hydrophobics. Additionally, sound speed propagation velocity, quality of building material index, elastic modulus and flexural strength were measured to evaluate the variation of mechanical properties. Static contact angle revealed that the coatings maintained an efficient level of hydrophobicity even after thermal-shock and freeze–thaw weathering tests. The study also revealed a critical interaction between freeze–thaw cycles, hydrophobic coatings and structural integrity of the stones, mostly on more porous ones. When they are subjected to harsh environmental conditions, untreated porous limestones keep structural cohesion, allowing for the natural absorption and release of water during freezing and thawing. On the contrary, when limestones are treated, the hydrophobic coatings can moderately obstruct the water release due to the partial saturation of the porous framework by the products. It also probably resulted from the different mechanical behavior between the inner matrix and layer of stone coated, resulting in a premature breakout and mechanical damage of the stone.



**Citation:** Lisci, C.; Sitzia, F.; Pires, V.; Mirão, J. Aging of Limestones and Silane–Siloxane-Based Protective Hydrophobics: The Impact of Heating–Cooling and Freeze–Thaw Cycles. *Heritage* **2024**, *7*, 6657–6682. <https://doi.org/10.3390/heritage7120308>

Academic Editor: Massimo Lazzari

Received: 8 October 2024

Revised: 17 November 2024

Accepted: 20 November 2024

Published: 26 November 2024

**Keywords:** limestone durability; coating durability; freeze–thaw cycles; thermal variation; physical–mechanical properties of limestones



**Copyright:** © 2024 by the authors. Licensee MDPI, Basel, Switzerland. This article is an open access article distributed under the terms and conditions of the Creative Commons Attribution (CC BY) license (<https://creativecommons.org/licenses/by/4.0/>).

## 1. Introduction

Stone is traditionally used in construction and architectural applications as a building element due to its aesthetic, technical properties and structural performance. As with other environmental factors (e.g., rain, humidity, moisture, salt presence, biological activity, etc.), heating–cooling and freeze–thaw cycles significantly undermine the longevity of stone materials [1,2] (Figure 1).

Persistent and abrupt heating–cooling cycles induce temperature gradients through the thickness of the stones. This is typical of continental climates and environments with high insolation at middle latitudes with humid–temperate climates where high-temperature variations are frequent [3]. Heating–cooling cycles occur in hot deserts with high-temperature fluctuations during the day (hot) and night (cold) [4]. Surface temperatures are also significantly affected by albedo, which plays a crucial role in determining the proportion of radiation-induced heat on the surface [5–7]. Another type of aging comparable to a thermal shock can take place during fire events where stones reach high-temperature exposure (thermal aging) with subsequent sudden cooling during the extinction with water [8,9].

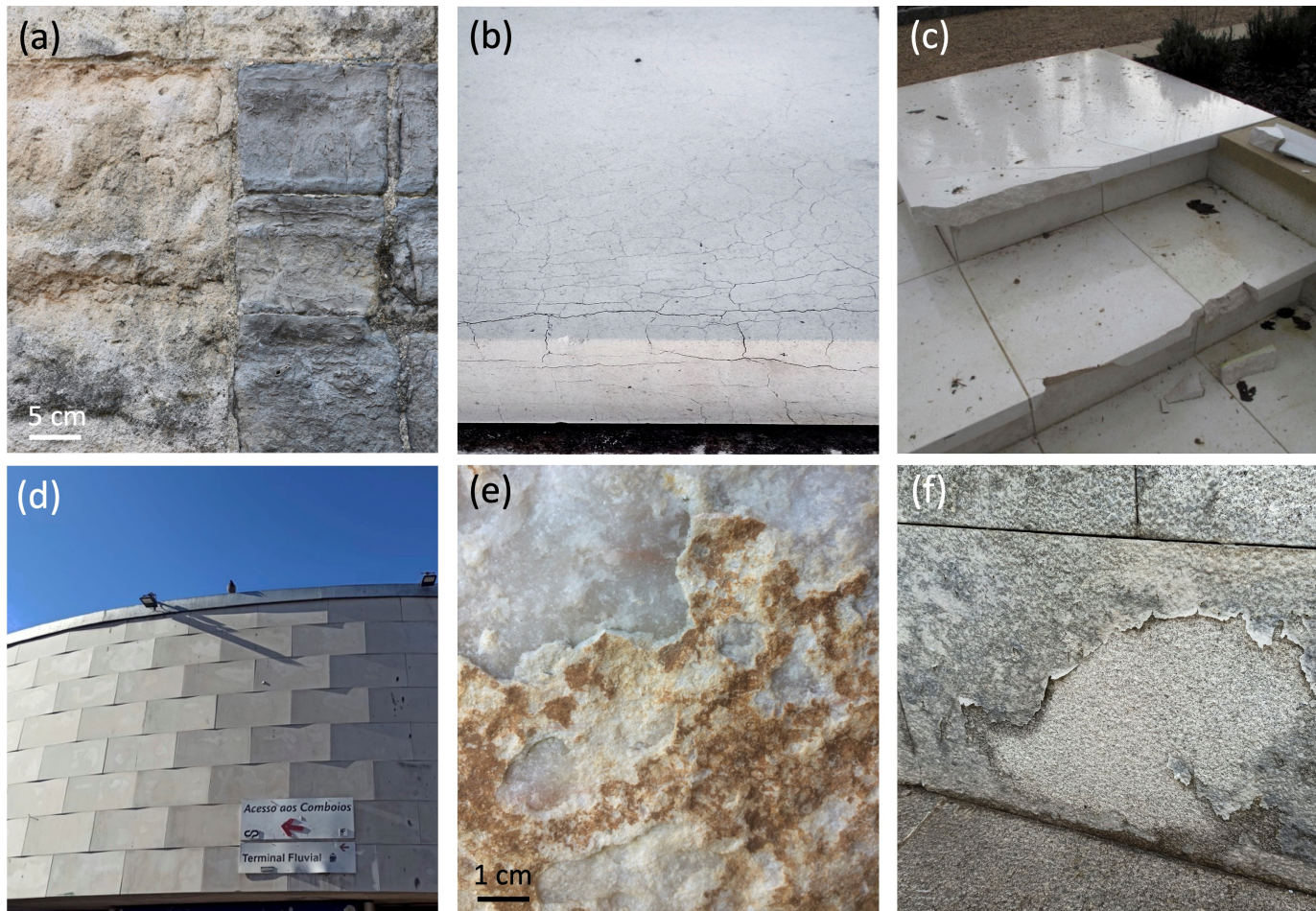


**Figure 1.** Common decay patterns and pathologies of stones subjected to heating–cooling (thermal shock) and freeze–thaw cycles: (a) masonry of Cardiff Castle (Cardiff, Wales (UK)—Köppen classification: Cfb climate, temperate oceanic climate or subtropical highland climate) presenting cracking of limestones and delamination of sandstones; (b) cracking due to freeze–thaw cycles of a limestone façade located in Memphis (USA) (Köppen classification: Cfa climate, humid subtropical climate); (c) fracturing and detachments of a Portuguese limestone pavement in New York (USA) (Köppen classification: Cfa climate, humid subtropical climate); (d) bowing of limestone cladding due to effect of heating–cooling cycles of the metro Cais do Sodré in Lisbon, Portugal (Köppen classification: Csa climate, warm-summer Mediterranean climate and hot-summer Mediterranean climate). Grazing late allows to detect the deformation and other defects of the façades. (e) Exfoliation of marble on a historic building due to thermal-shock aging in Vila Viçosa, Portugal (Köppen classification: Csa climate); (f) peeling of a coating applied on granite subjected to heating–cooling and wetting–drying cycles (Porto, Portugal—Csb climate).

Stones experience expansion and contraction as they absorb and release heat. The impact of surface temperatures is regulated by the thermal conductivity and specific heat capacity of the rock-forming minerals [10,11]. When they are subjected to temperature changes, thermal stress is caused by differential expansion and contraction of the minerals culminate in mechanical damage (i.e., granular disaggregation, cracking, spalling and detachments) [12]. This phenomenon is called “thermoclastism” and depends on the grain size of minerals and the texture of polycrystalline rocks. For example, in marble and granitic rocks, the size of crystals, boundaries and planes of weakness boost the thermoclastic damage [5]. In this case, the different linear coefficient of thermal expansion along the crystallographic axis of the minerals let the stone suffer decohesion, permanent deformation and brittle fracturing [13–15].

Freeze–thaw aging occurs in cold climates regions and in locations where the temperature fluctuates below zero degrees [16,17]. During freezing conditions, the water absorbed by the porous framework, through microcracks or other discontinuities expands up to 9% under atmospheric conditions [18], exerting a crystallization pressure on the solid fraction of the stone. Pure water typically freezes at the 0 °C transition under normal atmospheric conditions. However, in porous rocks, water can crystallize at temperatures lower than 0 °C. This can be attributed to either supercooling or a decrease in the freezing point. Supercooling occurs when temperature differences between the liquid film adjacent to the wall of an ice crystal pore and the temperature at which freezing reaches equilibrium [1,19]. Freeze point reduction emerges when the equilibrium conditions of the fluid change as salts are dissolved in water. In these circumstances, the primary cause of freeze point reduction in natural building stones is the distribution of pore space, pore size and pore distribution and interconnection, leading to freezing at progressively lower temperatures and in a heterogenous way [18,20,21]. When ice crystals form, they exert pressure on pore walls, potentially causing cracks. This pressure increases in smaller pores and colder conditions. Damage occurs either through immediate stress exceeding the material strength (critical failure) or over time from repeated cycles causing microcrack accumulation (sub-critical failure). The extent of damage depends on pore structure, water content, and the material tensile strength [22,23].

Furthermore, the frost action activates rock discontinuities like preexisting fractures, partially mineralized cracks or sedimentary bedding [24]. Reiterated freeze–thaw cycles weaken the stone, resulting in surface geometrical modification and deterioration, decohesion, and subsequent depletion of structural integrity and technical quality of the materials [1].

Heating–cooling cycles and freeze–thaw aging have destructive effects on stone materials because they reduce the load-bearing capacity, which is critical, especially in slabs for cladding, pavements and roofing with few mm thicknesses. Slabs generally bow and break down, and relative humidity, moisture, and other factors usually accelerate the aging and the onset of pathologies [25].

In stones with high open porosity, the effect of thermal stresses and freezing–thawing is aggravated since they absorb more water [26,27]. Furthermore, a high percentage of micropores are responsible for further damage where ice crystal growth easily exceeds the mechanical strength of the materials [28]. Freeze–thaw affects not only natural rocks but also engineered materials like concretes and ceramics. Understanding this process is crucial in the context of climate change, as shifts in temperature and moisture patterns may alter the extent of freeze–thaw impacts in some regions. Ice formation in porous materials generates internal stresses that can surpass the tensile strength of the material, leading to damage.

Several preventive measures can be implemented to minimize the impact of heating–cooling cycles and freeze–thaw aging on stones. Proper stone sustainable selection based on its porosity, resistance to temperature variations and freezing is essential. Surface treatments, particularly hydrophobic coatings, can be applied to provide a limitation

against liquid water infiltration. Inspections, maintenance, and repair intervention should be conducted regularly for ensuring the durability and performance requirements.

This work aims to determine the stone longevity and the durability of silane and siloxane-based hydrophobic coatings applied to limestones installed in environments where heating–cooling and free–thaw dominate. The assessment is conducted through laboratory salt weathering tests, following the principles set by the European standards EN 14066:2013 (determination of resistance to thermal shock [29]) and by EN 12371:2010 (determination of resistance to freezing–thawing [30]).

## 2. Materials and Methods

### 2.1. Building Stones

For the investigation, three important Portuguese limestones were selected from Estremadura Calcareous Massif (i.e., Branco, Alpinina, and Blue limestone) and one lithology (Lioz) quarried in Lisbon District (Figure 2).

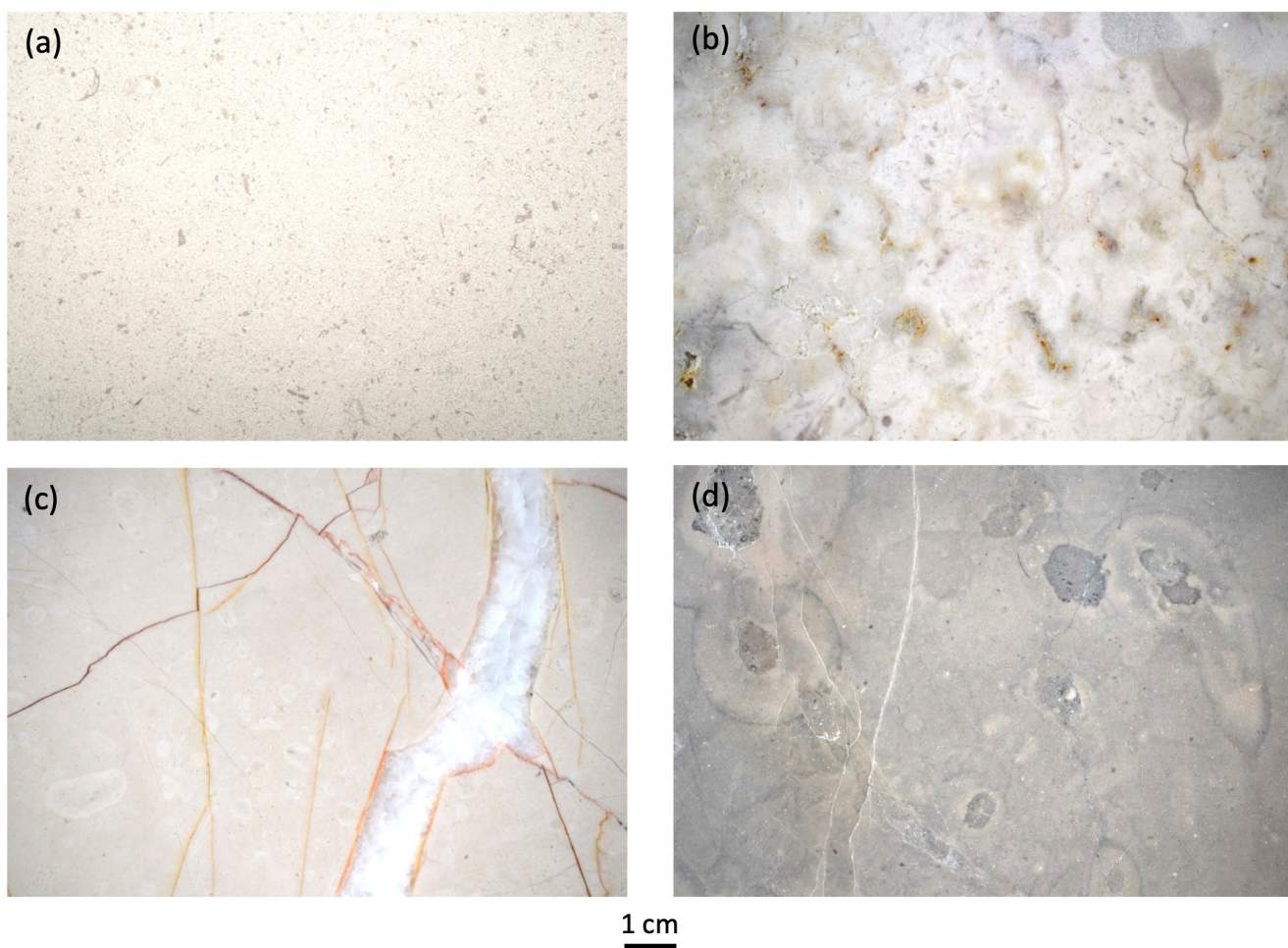


**Figure 2.** Macroscopic features of the selected limestones: (a) Branco; (b) Lioz; (c) Alpinina; (d) Blue limestone.

These stones are used in contemporary and ancient architecture. In particular, Lioz is listed as “Heritage Stone” by the IUGS, the International commission on Geoheritage.

Branco is a pure, soft limestone that ranges in color from cream to light cream. It is characterized by abundant bioclasts and oolites (Figure 2a).

Lioz is a coarse, very compact bioclastic limestone with an ivory-whitish color. It is identified by stylolitic joints, which vary in their opening and spacing depending on the facies (Figure 2b).

Alpinina is a very compact, fine-grained limestone with a light crème-beige color. It exhibits closed iron-rich stylolites and calcitic veins (Figure 2c).

Blue limestone is a massive bioclastic limestone with a grey-blue color. It contains a significant amount of organic matter, and it exhibits a low frequency of open/closed stylolites (Figure 2d).

Branco limestone is characterized by a grain-supported texture and the presence of oolites and peloids with interstitial sparite. Based on Folk classification [31], the rock can be considered an intermediate bio-ool-pelsparite (Figure 3a).

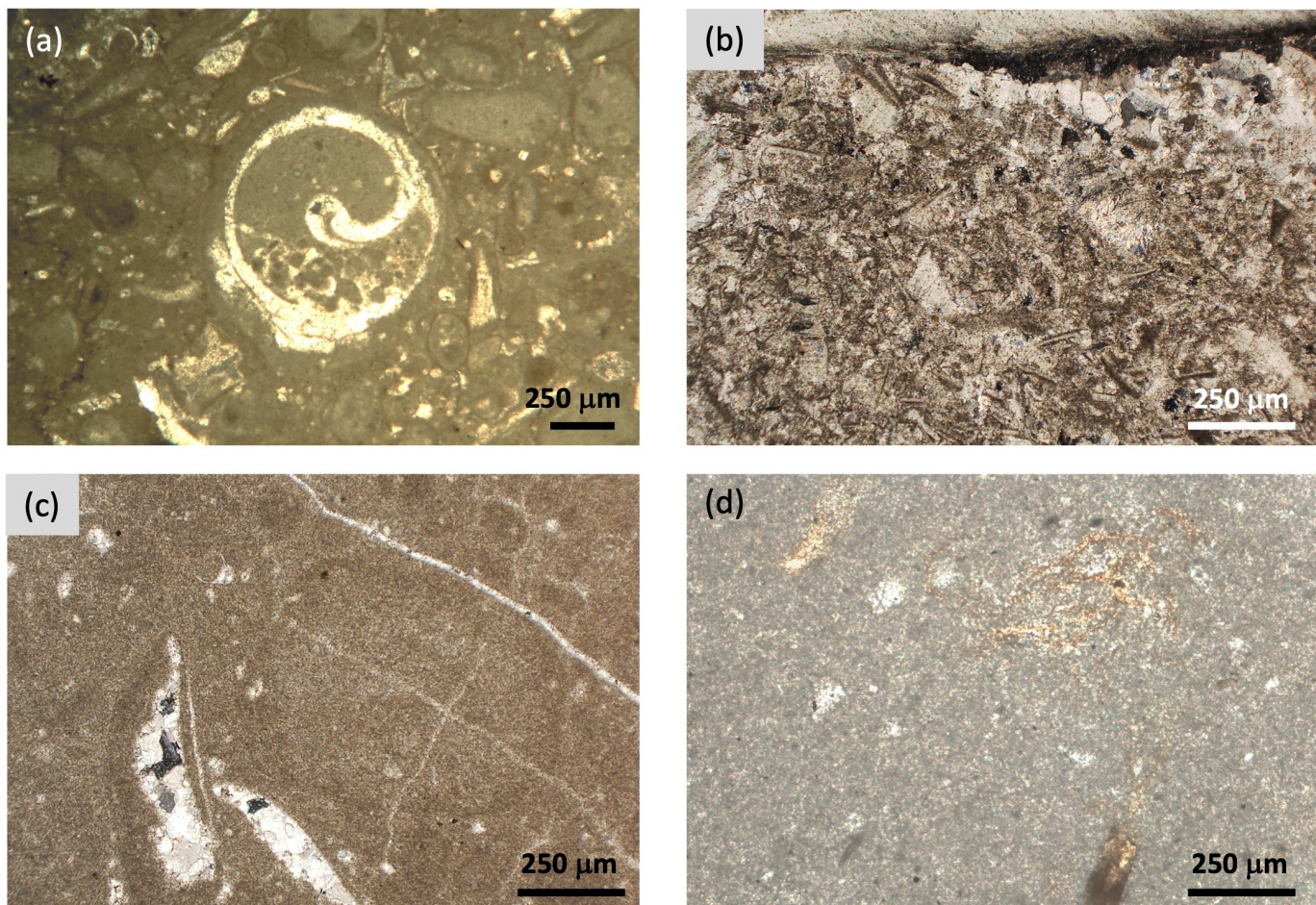


**Figure 3.** Thin section images and petrography of (a) Branco (bio-ool-pelsparite); (b) Lioz (biosparite); (c) Alpinina (pel-bioclastic-sparite); (d) Blue limestone (biomicrite).

Lioz presents a microcrystalline grain-supported texture. It has 52% of sparitic cement and about 48% of bioclasts. According to Folk, the rock is classified as biosparite (Figure 3b).

Alpinina has a mud-supported matrix. The matrix occupies about 80% of the thin section. A total of 10% belongs to recrystallized calcite (sparite) veins with openings from 0.1 mm up to 5 mm. Bioclasts and peloids represent the other 10%. According to Folk classification, Alpinina is a Pel-bioclastic-sparite (Figure 3c).

Blue limestone is characterized by over 90% vol. of a micritic matrix containing a low percentage (<2% vol) of clay minerals. The stone is marked by the abundant presence of organic matter up to 7% vol. Allochems of quartz (~1%) have also been detected. The bioclastic component is also relevant. According to Folk classification, the stone is classified as biomicrite (Figure 3d).

The main physical/mechanical characteristics of Branco, Lioz, Alpinina and Blue limestone are reported in Table 1.

**Table 1.** Value of bulk density, open porosity, and thermal conductivity of the limestones under study.

Lithotype	Bulk Density (g/cm <sup>3</sup> )	Open Porosity (%)	Thermal Conductivity ( $\lambda$ ) (W/m.K)
Branco	2.36 ± 0.03	12.7 ± 0.76	1.7 ± 0.02
Lioz	2.7 ± 0.01	0.44 ± 0.09	2.8 ± 0.04
Alpinina	2.7 ± 0	0.22 ± 0.02	2.8 ± 0.04
Blue limestone	2.69 ± 0	1.37 ± 0.16	2.5 ± 0.13

The specimens came into our laboratory already cut to size from the industry.

## 2.2. *Hydrophobic Coatings*

For each stone, according to EN 16581 (Conservation of Cultural Heritage—surface protection for porous inorganic materials—laboratory test methods for the evaluation of the performance of water repellent products) [32], 3 bulk samples for each lithology and each setting (untreated and treated stones) were used for each test.

A roll was used to apply the coating, ensuring complete saturation of the substrate of Branco and avoiding any excess of coating material on the lowest porous stones (Lioz, Alpinina, Blue limestone). The used hydrophobic are silica-based products, silane and siloxane.

Silanes are small, low-viscosity molecules that penetrate surfaces deeply and form durable covalent bonds with inorganic substrates, forming durable bonds that enhance the hydrophobic properties [33,34]. Their performance depends on the radical group and substrate type. Siloxanes, larger in size and with Si–O–Si chains, cure faster but have shallower penetration, making them ideal for porous substrates like natural stone. Silanes can also form stable bonds with oxides of aluminum, zirconium, tin, titanium, and nickel, which improve corrosion resistance and more durability [35,36].

The samples treated with aminopropyltriethoxysilane were labeled as “COATING 1”, and those coated with aminefluorosilane were labeled as “COATING 2”. Specimens treated with a methylmethoxysilane-based formulation were named “COATING 3”. In Tables 2–4, the information of the commercial products is available.

**Table 2.** Specifics of aminopropyltriethoxysilane (COATING 1).

Product Info	Value	Measurement Units
Type of product	Monocomponent	-
Specific weight	0.82 ± 0.05	kg/L
Consume	0.2–0.4	L/m <sup>2</sup>
Dry residue	7 ± 2	%
Color	Incolor	-
Solvent	Xilene	-
pH	-	-

**Table 3.** Specifics of fluorosilane (COATING 2). N.A. = not available.

Product Info	Value	Measurement Units
Type of product	Monocomponent	-
Specific weight	N.A.	-
Consume	10–30	mL/m <sup>2</sup>
Dry residue	N.A.	-
Color	Incolor	-
Solvent	Water	-
pH	N.A.	-

**Table 4.** Specifics of methylmethoxysilane (COATING 3). N.A. = not available.

Product Info	Value	Measurement Units
Type of product	Monocomponent	-
Specific weight	1.01	kg/L
Consume	0.50–0.2	L/m <sup>2</sup>
Dry residue	N.A.	-
Color	Light yellow	-
Solvent	Water	-
pH	5.8 at 20 °C	-

**2.3. Natural Stone Test Methods: EN 14066:2013—Determination of Resistance to Aging by Thermal Shock and EN 12371:2010 Determination of Frost Resistance**

EN 14066:2014 is the European standard for evaluating stones resistance and durability to thermal-shock aging. After the preparation, specimens of  $30 \times 5 \times 5$  cm were subjected to 20 cycles of heating–cooling (thermal shock). Each cycle included the following:

- (i) A total of 18 h ( $\pm 1$ ) of drying in a ventilated oven at  $70 \pm 5$  °C.
- (ii) A total of 6 h ( $\pm 1$ ) of immediate immersion in cool water at  $20 \pm 5$  °C.

EN 12371:2010 is the European standard for evaluating stone resistance and durability to freeze–thaw cycles. After preparation, specimens of  $30 \times 5 \times 5$  cm were subjected to 56 cycles of freeze–thaw. One cycle consisted of the following:

- (i) A total of 6 h of freezing in air with different steps of decreasing temperature down to  $-12$  °C.
- (ii) A total of 6 h of thawing of the samples immersed in water at  $20$  °C. This ensured water absorption, which would freeze during the next freeze cycle.

In Table 5, several available studies about the application of the European Standards on protected stones are presented, including the authors' methodologies. The lack of an extensive international bibliography regarding the utilization of the standard to assess the durability of stones protected with hydrophobics has been found, mostly concerning EN 14066 (thermal shock). Many researchers, including the authors, think that filling the gap by generating new data and insights is fundamental, as well as exploring the limits and advantages of standard principles [16,37,38].

**Table 5.** State of the art of EN 14066 and EN 12371 (thermal-shock/heating–cooling cycles and freeze–thaw aging) standards for natural stone affected by abrupt thermal variation. Lithology, the chemistry of hydrophobic coatings, and application methods, when declared, are also reported. Finally, the insights of these investigations are commented on.

References	Methodology	Samples	Substrate	Coating and Application Method	Outcome
Ugur, I., 2014 [39]	EN 14066:2004 Drying at $105$ °C then cooled in water at $20$ °C.	$5 \times 5 \times 2$ cm	Welded ignimbrite from Turkey	Waterborne fluorinated polysiloxane: Baygard RT®. immersion for 5 min.	Positive
Lisci et al., current study	EN 14066:2014 Drying at $70$ °C then cooled in water at $20$ °C.	Prisms of $30 \times 5 \times 5$ cm	Branco, Lioz, Alpinina, Blue limestone from Portugal	Aminopropyltriethoxysilane, aminefluorosilane, methylmethoxysilane, application by brushing	Overall Positive in terms of retaining hydrophobicity.
Striani et al., 2016 [40]	EN 12371:2003	Cubic specimens of 7 cm	Lecce stone: calcarenite	Organic–inorganic hybrid coating: HYBRIDSUN	Positive after 25 cycles

**Table 5.** Cont.

References	Methodology	Samples	Substrate	Coating and Application Method	Outcome
Di Benedetto et al., 2012	EN 12371:2010	Cubic specimens of 5 cm	Neapolitan Yellow volcanic tuff; Vicenza Stone limestone	Tetramethylenediammonium dichloride, application by immersion	Overall positive
Durmekova et al., 2021 [41]	EN 12371:2010	Cubic specimens of 5 cm	Volcanic tuff from Tuscany	Siloxane resin: Antipluvio S	Need improvement
Lisci et al., current study	EN 12371:2010	Prisms of 30 × 5 × 5 cm	Branco, Lioz, Alpinina, Blue limestone from Portugal	Aminopropyltriethoxysilane, aminefluorosilane, methylmethoxysilane, application by brushing	Overall Positive in terms of retaining hydrophobicity. Structural damage observed

#### 2.4. Stone Characterization and Damage Assessment

Petrographic analyses were conducted using an optical polarized microscope Leica DM2500P (Leica Microsystems, Wetzlar-Germany), and a digital polarized microscope Hirox-01 (Hirox Europe, Limonest, France). Thin sections of 30  $\mu\text{m}$  in thickness were examined to identify mineralogical compositions and rock fabric.

Open porosity measurements before and after the durability tests were conducted according to the EN 1936:2008 standard [42]. Specimens were subjected to a vacuum of  $(2.0 \pm 0.7)$  kPa for 2 h  $\pm$  24 min and then saturated with distilled water under vacuum, remaining immersed for  $24 \pm 2$  h.

Non-destructive ultrasonic tests were performed to calculate the dynamic indexes and structural integrity of the limestones before and after the durability tests. The PUNDIT PL200 (Screening Eagle Technologies Proceq, Schwerzenbach-Zurich, Switzerland) with 54 kHz transducers was used to calculate the velocity of the longitudinal waves ( $V_p$ ) according to EN 14579:2004 [43]. Using these values, the velocity ratio index (VRI, Equation (1)) was calculated:

$$\text{VRI} = (V_{pf}/V_{pi})^{0.5} \quad (1)$$

This index allowed for the measurement of the quality of building materials (Table 6) proposed by Kahraman [44], which is also adopted by other researchers in the application of NDT integrated techniques [45,46].  $V_{pf}$  represents the final velocity value after the test, and  $V_{pi}$  is the initial value of  $V_{pf}$  of the intact specimens.

**Table 6.** Quality of building materials according to the velocity ratio index (VRI) proposed by Kaharaman.

Quality of Building Materials	
VRI < 0.25	Very poor
0.25 < VRI < 0.50	Poor
0.50 < VRI < 0.75	Fair
0.75 < VRI < 0.90	Good
VRI > 0.90	Very good

The determination of the dynamic modulus of elasticity by measuring the fundamental resonance frequency in longitudinal vibration was achieved following EN 14146:2006 [47]. The value is then expressed in GPa. The equipment used was the ERUDITE MKII resonant frequency test system by C.N.S Electronics (Wallsend, United Kingdom) oupled with the digital storage oscilloscope UTD2025CL.

Flexural strength ( $\sigma_f$ ) was assessed through uniaxial compression tests following EN 12372:2008 [48]. A PEGASIL by Zipor with a load capacity of 25 kN was used to apply the rupture load perpendicular to the stratification planes or other discontinuities.

### 3. Results and Discussion

#### 3.1. Damage Assessment

##### 3.1.1. Visual Inspection

Visual inspection is essential to determine the overall macroscopic aspect and bulk integrity of the stones, such as noticeable color changes and morphological characterization for classifying the alteration/decay patterns (Figure 4).



**Figure 4.** Morphological changes of Branco, Lioz, Alpinina, and Blue limestone after EN 14066 (thermal-shock/heating–cooling cycles) and after EN 12371 (freeze–thaw aging). No evident color changes in the stones were noticed. Slight rounding was noticed on Branco.

EN 16140:2013 [49] imposes the determination of sensitivity to changes in appearance produced by thermal cycles. No evident color changes were noticed imputable to oxidation, chemical alteration or any degradation of the hydrophobic protectives. The code of the stones (or class), from T1 to T3, according to the oxidation degree is evaluated, where T1 means that no oxidation happened.

Morphological changes of Alpinina and Blue limestone after EN 14066 (thermal-shock/heating–cooling cycles) and after EN 12371 (freeze–thaw aging) were not so evident. Contrary, on Branco and Lioz after EN 12371, a rounding of edges and corners was detected. In samples of Branco treated with hydrophobics, micro and major cracks with different propagation and openings appeared (Figure 5).

TREATED BRANCO  
AFTER EN 12371

Detail of a 30 × 5 × 5 cm prism



**Figure 5.** In some prismatic samples of Branco treated with hydrophobics, fractures with different propagation and openings appeared.

EN 12371 proposes a more complex rating for classifying the structural integrity of the stones based on morphological variation after freeze–thaw cycles (Table 7). Visual inspection was executed each day, and the first deterioration patterns were recognized at the 15th cycle on Branco, with the great damage identified after 30 cycles on most of the treated samples.

**Table 7.** Rating of stones after 56 cycles, based on visual inspection and detection of minor and major damage after freeze–thaw cycles specified in EN 12371. No damage was observed after EN 14066. After EN 12371, slight rounding of edges and corners was detected on untreated Branco and Lioz samples, to which a score = 1 was attributed. Regarding the samples treated with hydrophobic coatings, a score equal to 3 and 4 can be featured in Branco samples, testifying to the weakness of the stone. COATING 1 = aminopropyltriethoxysilane; COATING 2 = aminefluorosilane; COATING 3 = methylmethoxysilane-based formulation.

Score	Classification	Untreated Samples	COATING 1	COATING 2	COATING 3
0	Specimen intact	All samples are intact after EN 14066 All Lioz, Alpinina, Blue limestone samples (treated and untreated)	All samples are intact after EN 14066 After EN 12371: All Lioz, Alpinina, Blue limestone samples	All samples are intact after EN 14066 After EN 12371: All Lioz, Alpinina, Blue limestone samples	All samples are intact after EN 14066 After EN 12371: all Lioz, Alpinina, Blue limestone samples
1	Very minor damage (minor rounding of corners and edges), which does not compromise the integrity of the specimen	Untreated Branco and Lioz samples after EN 14066 and after EN 12371.			
2	One or several micro-cracks (<0.1 mm width) or detachment of small fragments (<30 mm <sup>2</sup> per fragment)		Detected in all Branco specimens	Detected in all Branco specimens	Detected in all Branco specimens
3	One or several cracks, holes or detachments of fragments larger than those defined for the “2” rating, or alteration of materials in veins, or the specimen shows important signs of crumbling or dissolution		Detected in two samples of Branco treated with COATING 1 and after EN 12371	Detected in 2 samples of Branco treated with COATING 2 and after EN 12371	Detected in 1 samples of Branco treated with COATING 3 and after EN 12371
4	Specimen with major cracks or broken in two or more or disintegrated		Detected in one sample treated with Branco COATING 2 and after EN 12371	Detected in one sample treated with Branco COATING 2 and after EN 12371	Detected in two samples of Branco treated with COATING 3 and after EN 12371

### 3.1.2. Wettability and Static Contact Angle

Wettability is a property that expresses the spreading of a liquid on a solid surface, and the static contact angle measures it. The static contact angle is the angle between the solid/liquid interface and the liquid/vapor interface when the solid, liquid, and vapor phases are in equilibrium. The equilibrium angle is called the Young contact angle [50]. In the case of measurement of a liquid drop spreading on a horizontal surface, the angle is defined as “static contact angle”. When the liquid drops on an inclined surface, it is defined as “dynamic contact angle” or “roll off” angle. As water is the main agent of chemical weathering, the application of protective coatings inhibits the electrostatic attraction between the water polar molecules and the electronegative groups of stones, mostly

carbonate and silicate [51], installed in outdoor environments or in indoor environment with extensive moisture formation on the surface of materials. Hence, the application of hydrophobics helps to increase the surface tension of the water (or any liquid), so cohesive forces between the molecules of the liquid are intensified. In parallel, the surface free energy of the solid is reduced to a minimum, and the solid surface resists the wetting by water/liquids. The surface free energy expresses the excess of energy due to the imbalance between forces generated by contact between two different thermodynamic phases, such as solid/liquid/gas [52] (Figure 6).

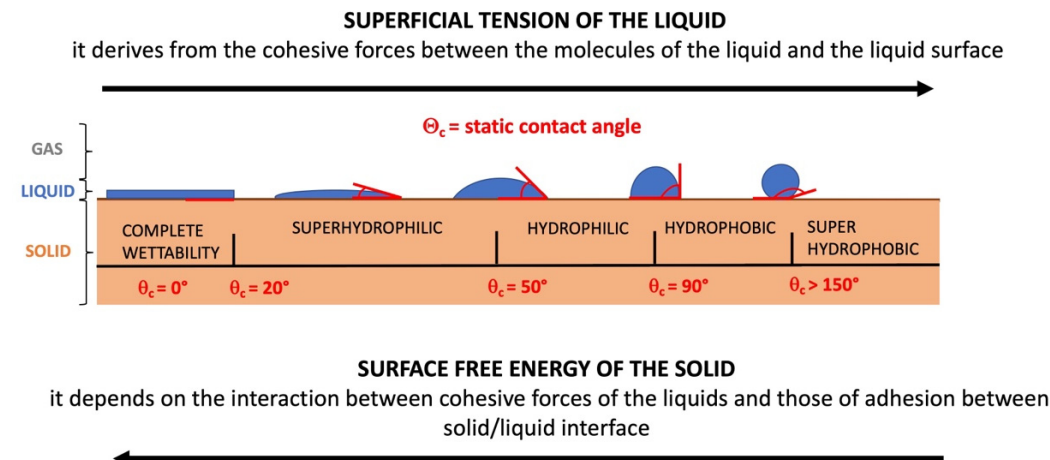


**Figure 6.** Simplified schematic representation of the relationship between contact angle, surface tension, free surface energy of the solid and wettability.

In Table 8, values of static contact angle ( $\Theta^\circ$ ) determined before heating–cooling cycles (thermal shock, EN 14066) and freeze–thaw cycles (EN 12371) are listed and discussed.

**Table 8.** Minimum and maximum contact angle values expressed in degrees ( $\Theta^\circ$ ) for each lithotype, both for untreated stones and those with coatings. A total of 10 measures were made in each sample. COATING 1 = aminopropyltriethoxysilane; COATING 2 = aminefluorosilane; COATING 3 = methylmethoxysilane-based formulation. For more porous stones, such as untreated Branco and Blue limestone, an initial contact angle ( $\Theta^\circ$ ) of 0 indicates that water fully permeated the stones either immediately or within a very short time. In contrast, for low-porosity stones like Alpinina and Lioz, a  $\Theta^\circ$  of 0 means that water quickly spread across the stone surface and remained in contact with it for a longer duration.

Sample	Pre-Test ( $\Theta^\circ$ )		After EN 14066 ( $\Theta^\circ$ )		After EN 12371 ( $\Theta^\circ$ )	
	Min	Max	Min	Max	Min	Max
Branco Untreated	0	0	0	0	0	0
Branco COATING 1	114	117	80	98	99	114
Branco COATING 2	126	128	87	100	100	124
Branco COATING 3	130	135	87	103	95	110

**Table 8.** *Cont.*

Sample	Pre-Test ( $\Theta^\circ$ )		After EN 14066 ( $\Theta^\circ$ )		After EN 12371 ( $\Theta^\circ$ )	
	Min	Max	Min	Max	Min	Max
Lioz Untreated	0	0	0	0	0	0
Lioz COATING 1	113	118	90	106	80 Close to stylolites	120
Lioz COATING 2	121	126	97	110	89 Close to stylolites	103
Lioz COATING 3	134	138	109	118	95	130
Alpinina Untreated	0	0	0	0	0	0
Alpinina COATING 1	112	117	88	115	55	61
Alpinina COATING 2	131	136	88	106	127	133
Alpinina COATING 3	133	138	85	114	130	136
Blue limestone Untreated	0	0	0	0	0	0
Blue limestone COATING 1	110	116	103	111	77	92
Blue limestone COATING 2	122	128	99	112	97	119
Blue limestone COATING 3	130	135	85	96	95	120

### Branco Results

The untreated samples had complete wettability before and after the tests. The samples treated with COATING 1 (aminopropyltriethoxysilane) had a static contact angle ( $\Theta^\circ$ ) pre-test ranging from  $114^\circ$  to  $117^\circ$ , and from  $80^\circ$  to  $98^\circ$  after EN 14066 (thermal shock).  $\Theta^\circ$  increased from  $99^\circ$  to  $114^\circ$  after EN 12371. COATING 2 (aminefluorosilane) and COATING 3 (methylmethoxysilane) performed similarly after EN 14066, with contact angle values ranging from  $87^\circ$  to  $100^\circ$  (COATING 2) and from  $87^\circ$  to  $103^\circ$  (COATING 3). All minimum values were below  $<90^\circ$ , but considering the entity of the aging, the authors think the results are satisfactory. After EN 12371 (freeze–thaw), all minimum values of  $\Theta^\circ$  were above  $90^\circ$ , and COATING 2 presented the best performance, with a contact angle ranging from  $100^\circ$  to  $124^\circ$ , followed by COATING 1 and COATING 3, respectively.

### Lioz Results

Water spread rapidly on the surface of the untreated samples, reaching  $0^\circ$  quickly.  $\Theta^\circ$  measured in COATING 1 samples decreased from  $113^\circ$ – $118^\circ$  (pre-test) to  $90^\circ < \Theta^\circ < 106^\circ$  after modified EN 14066, and  $80^\circ < \Theta^\circ < 120^\circ$  after EN 12371. A value of  $80^\circ$  was detected next to a stylolite, where the ice pressure controlled the opening of the discontinuities and the propagation of microcracks. Propagation of microcracks, subsequently, involved the degradation of the coating.

Regarding COATING 2, the degree of hydrophobicity was good after EN 14066, with  $97^\circ < \Theta^\circ < 110^\circ$ . COATING 2 suffered more from the effect of freeze–thaw aging (EN 12371), with the static contact angle in the range  $89^\circ$ – $103^\circ$ . Finally, COATING 3

showed similar behavior, but the decrease in  $\Theta^\circ$  with respect to the initial values was substantial after thermal-shock aging (EN 14066). After EN 12371, in some portions of the stone,  $\Theta^\circ$  was measured up to 130°, while the minimum value obtained was 95°. This means that COATING 3 was more sensitive to high thermal variations caused by heating–cooling cycles.

#### Alpinina Results

On untreated samples, water spread rapidly on the surface, so the value pre-test achieved 0° in a few seconds. In general, all coated Alpinina samples similarly suffered the heating–cooling cycles that occurred during the application of EN 14066, with minimum values of 85° (COATING 3) <  $\Theta^\circ$  < 88° (COATING 1 and COATING 2). Furthermore, COATING 2 and COATING 3 revealed satisfactory behavior when subjected to freeze–thaw cycles (EN 12371), with the lowest  $\Theta^\circ$  detected equal to 127°–130°. COATING 1, with values below the hydrophobicity level (55°–61°), showed a greater degradation of the product and greater vulnerability to low temperatures.

#### Blue Limestone Results

Positive results refer to COATING 2, where both EN 14066 and EN 12371 static contact angles proved the efficiency of this product applied on that limestone subjected to strong temperature variation. COATING 1 protected the stone in case of heating–cooling cycles, but after freeze–thaw, it suffered a substantial decrease in the minimum value of the contact angle, from  $\Theta^\circ = 110^\circ$  (pre-test) to  $\Theta^\circ = 77$  after the test. The maximum value calculated was  $\Theta^\circ = 92$ , slightly above the limit of hydrophobicity. On the other hand, COATING 3 better performed when exposed to freeze–thaw aging (EN 12371), testified by a static contact angle in the range 95° <  $\Theta^\circ$  < 120°.

#### 3.1.3. Variation of Mass and Open Porosity

Generally, concerning mass, expressed as a percentage ( $\Delta M\%$ , Table 9), marginal variation of the original mass was detected. No significant loss of material and detachments took place, even in Branco, where grain disaggregation on treated samples emerged. Only slight rounding and decohesion occurred without any conspicuous stone break-out, as also depicted previously in Figures 4 and 5 and Table 7. In Branco, the variation in open porosity ( $\Delta \Phi_0\%$ ) was substantial, mostly in Branco samples where the structural integrity was compromised, particularly after freeze–thaw cycles (EN 12371). Furthermore, low mass variation and open porosity were observed in the case of low-porosity stones such as Lioz and Alpinina and, sporadically, Blue limestone.

**Table 9.** Values of mass variation ( $\Delta M\%$ ) and open porosity ( $\Delta \Phi_0\%$ ) referring EN 14066 (thermal shock) and EN 12371 (freeze–thaw). COATING 1 = aminopropyltriethoxysilane; COATING 2 = aminefluorosilane; COATING 3 = methylmethoxysilane-based formulation.

Sample	$\Delta M\%$		$\Delta \Phi_0\%$	
	After EN 14066	After EN 12371	After EN 14066	After EN 12371
Branco Untreated	average	−0.02	−0.22	−4
	st.dev	±0.01	±0.05	±0.7
Branco COATING 1	average	−0.01	−0.26	15
	st.dev	-	±0.08	±8
Branco COATING 2	average	0.01	−0.26	34
	st.dev	-	±0.09	±18
Branco COATING 3	average	−0.01	−0.29	37
	st.dev	0.04	±0.04	±39

**Table 9.** *Cont.*

Sample	$\Delta M$ (%)		$\Delta \Phi_o$ (%)	
	After EN 14066	After EN 12371	After EN 14066	After EN 12371
Lioz Untreated	average	−0.02	−0.03	−7
	st.dev	−	±0.002	±24
Lioz COATING 1	average	−0.02	−0.03	22
	st.dev	−	±0.03	±0.77
Lioz COATING 2	average	−0.002	−0.04	8.5
	st.dev	±0.02	±0.01	±0.67
Lioz COATING 3	average	−0.05	−0.22	48
	st.dev	±0.01	±0.05	±45
Alpinina Untreated	average	−0.02	0.01	−18
	st.dev	±0.06	−	±26.4
Alpinina COATING 1	average	−0.02	0.1	4
	st.dev	±0.06	±0.005	±39
Alpinina COATING 2	average	−0.02	0.1	−12
	st.dev	±0.06	±0.002	±27
Alpinina COATING 3	average	−0.02	0.01	6
	st.dev	−	±0.004	±27
Blue limestone Untreated	average	−0.02	−0.04	7
	st.dev	±0.1	±0.002	±7
Blue limestone COATING 1	average	−0.02	0.02	3
	st.dev	±0.06	±0.11	±5
Blue limestone COATING 2	average	−0.02	−0.03	28
	st.dev	±0.06	±0.003	±17
Blue limestone COATING 3	average	−0.02	−0.03	12
	st.dev	±0.06	±0.001	±9

### Branco Results

Untreated samples showed a  $-4 \pm 0.7 < \Delta \Phi_o \% < 4 \pm 5$ , after EN 14066 and after EN 12371, respectively. Unexpectedly, all treated samples suffered a huge variation in porosity. After EN 14066, they encountered an increase in porosity between  $15 \pm 8$  (COATING 1)  $< \Delta \Phi_o \% < 37 \pm 39$  (COATING 3), being  $\Delta \Phi_o \%$  of COATING 2 equal to  $34 \pm 39$ . After EN 12371, the substantial variation of open porosity reaches the value of  $733 \pm 192\%$  in the case of COATING 3,  $553 \pm 74\%$  refers to the samples treated with COATING 2 and, finally, COATING 1 presented  $\Delta \Phi_o$  average =  $534 \pm 19\%$ . As can be noticed, the standard deviation after the durability tests also indicates the large variability of the extent of structural damage experienced by each sample.

### Lioz Results

Untreated samples have undergone small  $\Delta M$  variation after EN 14066.

Variation of open porosity ( $\Delta \Phi_o \%$ ) increased after the performance of EN 12371 on treated samples. Standard deviation is also higher with respect to the untreated samples, representing the variability of the results related to the structural heterogeneities of the lithology, which confer different responses to the heating–cooling and freeze–thaw cycles. After 14066,  $\Delta \Phi_o$  ranges from  $-7 \pm 24\%$  (untreated samples) to  $48 \pm 45\%$  on COATING 3, with COATING 2 represented by  $\Delta \Phi_o = 8.5 \pm 0.67\%$  and COATING 1 by  $\Delta \Phi_o = 22 \pm 0.77\%$ .

After EN 12371, untreated Lioz COATING 1 gave  $\Delta\Phi_o = 47 \pm 42\%$ , followed by COATING 3 ( $\Delta\Phi_o = 52 \pm 48\%$ ) and COATING 2 ( $\Delta\Phi_o = 80 \pm 44\%$ ).

#### Alpinina Results

The very low porous Alpinina Lioz experienced  $\Delta\Phi_o$  ranging from  $-18\%$  (untreated) to  $6\%$  (COATING 3) after thermal-shock cycles (EN 14066). Regarding COATING 2  $\Delta\Phi_o = 101\%$ , in the case of COATING 1  $\Delta\Phi_o = 68\%$  and COATING 3 have shown  $\Delta\Phi_o = 33\%$ , while on the untreated samples, an  $\Delta\Phi_o = 24\%$  was calculated.

After freeze–thaw aging (EN 12371), the variation is higher in treated samples (as in Lioz and Branco), testifying that the protective coatings exposed to freeze–thaw could negatively affect the stone resistance at cold temperatures.

#### Blue Limestone Results

Regarding Blue limestone, the same consideration about the effect of thermal-shock and freeze–thaw cycles can be achieved: thermal shock was less harmful than freezing–thawing in changing open porosity. In general, except for the samples treated with COATING 1 ( $\Delta\Phi_o = 3 \pm 5\%$ ), treated specimens were more affected by thermal variation after EN 14066. COATING 2 exhibited  $\Delta\Phi_o = 28 \pm 17\%$ , COATING 3  $\Delta\Phi_o = 12 \pm 9\%$ , while untreated Blue limestone  $\Delta\Phi_o = 7 \pm 7\%$ .

After EN 12371,  $\Delta\Phi_o$  was lower in untreated samples ( $15 \pm 9\%$ ). In COATING 1,  $\Delta\Phi_o = 45 \pm 5\%$ ; regarding COATING 2,  $\Delta\Phi_o = 53 \pm 16\%$ . The same values were calculated for COATING 3, with  $\Delta\Phi_o = 52 \pm 16\%$ .

It is noteworthy that hydrophobic treatments exhibit efficacy in mitigating water absorption, as detected by the static contact angle.

When subjected to freeze–thaw cycles (EN 12371), stones (especially highly porous stones like Branco) undergo microcracking and disaggregation, enabling water access. Hydrophobic coatings penetrate the inner porous matrix, probably impeding the regular release of water absorbed through microcracks/fractures during thawing. Consequently, over successive cycles, a larger volume of water is subjected to freezing inside the stone, causing ice volume expansion within the porous framework. This expansion induces a generalized internal crystallization pressure, resulting in more pronounced damage with respect to the untreated ones. In fact, as seen in the visual inspection paragraph (Figure 4), untreated Branco samples do not display evident structural decohesion. The absence of hydrophobic products permitted water to be naturally absorbed and subsequently thawed. Consequently, the internal pressure exerted by ice during freezing cycles is comparatively lower and prevented in untreated stones. Moreover, a different mechanical behavior between untreated inner matrix and the exposed treated matrix/coating layer could be the reason for the strong breakout and mechanical damage of the stone.

In the case of thermal shock (EN 14066), the difference between untreated and treated stones is less marked because of the non-occurrence of freezing and non-existence of ice crystallization pressure. Nevertheless, due to differential expansion and contraction during abrupt temperature fluctuations, minerals experience rapid and drastic temperature changes according to their thermal properties, provoking thermal stresses within the material.

Although bibliographic research was conducted to verify similar interpretations and probe them within the existing literature, the specific influence of hydrophobic coatings on the mechanical different behavior of stone materials during freeze–thaw and thermal-shock cycles remains deeply unexplored.

#### 3.1.4. Non-Destructive Testing: Ultrasound Velocity and Elastic Modulus

Measurement of mechanical properties by non-destructive way in the laboratory allowed the assessment of the quality of the stone by detecting any weakness and the contribution of microcracks, cracks, fracturing, and any other discontinuities that determine the type of decay. Before and after the durability tests (Tables 10 and 11), values of

longitudinal pulse velocity and its variation ( $V_p$  and  $\Delta V_p\%$ ) were measured, as well as the quality of building materials measured on the base of  $V_p$  (QBM), elastic modulus expressed in GPa (E), and its variation  $\Delta E\%$ .

**Table 10.** Dynamic and elastic properties of the stones before and after thermal-shock cycles (EN 14066 standard): longitudinal pulse velocity and its variation ( $V_p$  and  $\Delta V_p\%$ ); quality of building materials measured on the base of  $V_p$  (QBM), elastic modulus expressed in GPa (E) and its variation  $\Delta E\%$ ). Blue l = Blue limestone. COATING 1 = aminopropyltriethoxysilane; COATING 2 = aminefluorosilane; COATING 3 = methylmethoxysilane-based formulation.

EN 14066								
Sample		$V_p$ Before Test (m/s)	$V_p$ After Test (m/s)	$\Delta V_p\%$ (%)	QBM	E (GPa) Before Test	E (GPa) After Test	$\Delta E\%$ (%)
Branco Untreated	average	3928	3681	−6	QBM 0.98 = very good	31.154	28.215	−9
	st.dev	±316	±404			±4.970	±4.871	
Branco COATING 1	average	3993	3865	−3	QBM 0.99 = very good	31.695	29.403	−7
	st.dev	±303	±345			±3.325	±2.300	
Branco COATING 2	average	3975	3865	−3	QBM 0.99 = very good	31.847	30.677	−4
	st.dev	±55	±38			±0.776	±0.854	
Branco COATING 3	average	4275	4103	−4	QBM 0.98 = very good	35.744	33.816	−5
	st.dev	±453	±343			±5.536	±5.062	
Lioz Untreated	average	6122	6160	1	QBM 1 = very good	77.371	77.992	1
	st.dev	±12	±13			±2.980	±0.095	
Lioz COATING 1	average	6127	6110	−2	QBM 0.99 = very good	79.454	77.935	−2
	st.dev	±26	±74			±0.401	±1.043	
Lioz COATING 2	average	6152	6023	−5	QBM 0.98 = very good	79.209	77.918	−2
	st.dev	±32	±185			±0.284	±0.479	
Lioz COATING 3	average	6114	6053	−2	QBM 0.99 = very good	77.996	77.880	−0.1
	st.dev	±31	±72			±0.917	±0.785	
Alpinina Untreated	average	6186	6174	−0.20	QBM 0.99 = very good	78.748	73.448	−7
	st.dev	±6	±24			±1.045	±2.564	
Alpinina COATING 1	average	6156	6131	−0.41	QBM 0.99 = very good	71.886	68.141	−5
	st.dev	±78	±75			±7.898	±8.807	
Alpinina COATING 2	average	6111	6024	−1.42	QBM 0.99 = very good	74.368	68.464	−8
	st.dev	±86	±184			±4.540	±7.827	
Alpinina COATING 3	average	6146	6059	−1.40	QBM 0.99 = very good	75.481	71.723	−5
	st.dev	±20	±69			±4.176	±5.804	
Blue l. Untreated	average	5833	5826	−0.10	QBM 0.99 = very good	74.143	64.497	−10
	st.dev	±6.54	±30			±0.386	±3.435	
Blue l. COATING 1	average	5833	5799	−0.58	QBM 0.99 = very good	70.586	60.08	−15
	st.dev	±33	±45			±1.187	±3.497	
Blue l. COATING 2	average	5883	5869	−0.23	QBM 0.99 = very good	72.926	66.433	−9
	st.dev	±61	±67			±0.627	±1.464	
Blue l. COATING 3	average	5814	5833	0.32	QBM 0.99 = very good	70.997	65.476	−8
	st.dev	±30	±34			±0.724	±1.793	

**Table 11.** Dynamic–elastic properties of the stones before and after freeze–thaw cycles (EN 12371 standard): longitudinal pulse velocity and its variation ( $V_p$  and  $\Delta V_p\%$ ); quality of building materials measured on the base of  $V_p$  (QBM); elastic modulus expressed in GPa (E) and its variation  $\Delta E\%$ ). Blue l = Blue limestone. COATING 1 = aminopropyltriethoxysilane; COATING 2 = aminefluorosilane; COATING 3 = methylmethoxysilane-based formulation.

EN 12371								
Sample		$V_p$ Before Test (m/s)	$V_p$ After Test (m/s)	$\Delta V_p\%$ (%)	QBM	E (GPa) Before Test	E (GPa) After Test	$\Delta E\%$ (%)
Branco Untreated	average	4572	3853	-16	QBM 0.92 = very good	40.151 ±2.903	27.037 ±7.804	-33
Branco COATING 1	average	4515	3376	-25	QBM 0.99 = very good	40.346 ±1.042	35.996 ±22.212	-11
Branco COATING 2	average	4659	3086	-34	QBM 0.86 = good	41.474 ±0.608	14.916 ±1.328	-64
Branco COATING 3	average	4503	2902	-36	QBM 0.81 = good	39.599 ±0.963	12.879 ±0.523	-67
Lioz Untreated	average	5630	5531	-2	QBM 0.99 = very good	69.082 ±6.022	65.859 ±5.557	-5
Lioz COATING 1	average	5901	5824	-1	QBM 1 = very good	72.441 ±1.651	71.068 ±1.321	-2
Lioz COATING 2	average	5734	5747	0.2	QBM 0.98 = very good	72.852 ±2.226	70.310 ±1.391	-3
Lioz COATING 3	average	5628	5523	-2	QBM 0.99 = very good	67.498 ±3.779	65.959 ±3.678	-2
Alpinina Untreated	average	6167	5663	-8	QBM 0.99 = very good	69.143 ±6.244	44.192 ±21.967	-36
Alpinina COATING 1	average	6061	5564	-8	QBM 0.99 = very good	59.152 ±16.189	50.045 ±21.434	-15
Alpinina COATING 2	average	6312	5807	-8	QBM 0.99 = very good	74.066 ±1.746	62.949 ±9.080	-15
Alpinina COATING 3	average	6196	5670	-8	QBM 0.99 = very good	70.776 ±8.030	58.889 ±3.143	-17
Blue l. Untreated	average	5953	5776	-3	QBM 0.98 = very good	69.379 ±4.311	65.842 ±8.727	-1
Blue l. COATING 1	average	5960	5751	-4	QBM 0.98 = very good	77.091 ±10.472	69.802 ±1.060	-9
Blue l. COATING 2	average	5956	5784	-3	QBM 0.98 = very good	71.268 ±1.828	70.302 ±2.172	-1
Blue l. COATING 3	average	5984	5769	-4	QBM 0.98 = very good	71.284 ±0.588	70.284 ±1.083	-1

No European standard specifies the toleration of variation, but EN 12371 of freeze–thaw cycles ask us to note any variation of 30%, which the authors also consider for the other properties.

### Branco Results

Regarding Branco limestone,  $\Delta V_p\%$  was between  $-6$  (untreated samples) and  $-4$  (COATING 3), with  $\Delta V_p\% = -3$  in COATING 1 and 2, after EN 14066 (Table 10).  $\Delta E\%$  was higher for untreated Branco ( $\Delta E\% = -9$ ). A small difference with respect to the untreated stones was calculated for COATING 1 ( $\Delta E\% = -7$ ). In COATING 2 and COATING 3,  $\Delta E\% = -4$  and  $-5$ , respectively.

After EN 12371 (Table 11), the difference is more pronounced (as porosity), and it ranges from  $\Delta V_p\% = -16$  of the untreated samples to  $\Delta V_p\% = -36$  of COATING 3. In COATING 2,  $\Delta V_p\% = -34$ , and in COATING 1,  $\Delta V_p\% = -25$ .

The elastic modulus (E) also confirmed that freeze–thaw affected the treated samples more. In COATING 2 and 3,  $\Delta E\% = -64$  and  $-67$ , respectively. In COATING 1,  $\Delta E\%$  was just equal to  $-11$ , but the standard deviation was much higher, at  $\pm 22.212$  GPa instead of  $\pm 1.328$  and  $\pm 0.523$  GPa of COATING 1 and 2, respectively. This indicates a wider variability of COATING 1 to be durable in conditions of freeze–thaw cycles. On the untreated samples,  $\Delta E\%$  suffered a decrease of  $\Delta E\% = -33$ .

The quality of building material associated with this stone was very good after both durability tests.

### Lioz Results

After EN 14066, the  $\Delta V_p\%$  of Lioz samples was in the range  $-5$  (COATING 2)  $< \Delta V_p\% < 1$  (untreated sample). The quality of building materials remained “very good”, contrary to what was expected by reading the data on the porosity of the same samples.

Similar considerations can be achieved by reading the results obtained after performing freeze–thaw cycles (EN 12371), with  $-2$  (untreated samples and COATING 3)  $< \Delta V_p\% < 0.2$  (COATING 2).

### Alpinina Results

After thermal shock (EN 14066), Alpinina is the lithotype that underwent less alteration in  $V_p$ , with about  $-1.4$  (COATING 2 and 3, respectively)  $< \Delta V_p\% < -0.2$  (untreated). In Alpinina, treated stones also experienced more variation in dynamic properties. Being a very low-porosity stone ( $\sim 0.2\%$ ), a depletion of  $V_p$  was not expected after thermal-shock cycles. On the other hand, minimum values of static contact angle and open porosity after EN 14066 demonstrated that even Alpinina can be highly susceptible to abrupt thermal variation.

Variation in elastic modulus  $\Delta E$  was more accentuated, and it decreased between  $-8\%$  (COATING 2),  $-5\%$  (COATING 1 and COATING 3), and  $-7\%$  in untreated samples.

A different behavior of Alpinina was discerned after EN 12371, with a higher  $\Delta V_p\%$  aligned to the harmful effect of freeze–thaw. Untreated samples presented a negative  $\Delta V_p\% = -8$  in all samples. Regarding the elastic modulus (E), a reduction of  $-36\%$  was calculated, which is about double the difference calculated in the other samples, with  $\Delta E\% = -15$  (COATING 1 and 2). In COATING 3,  $\Delta E\% = -17$ .

### Blue Limestone Results

This stone, together with the Alpinina, was less affected by the damage deriving from thermal shock. After EN 14066, the  $\Delta V_p\%$  is  $-0.58$  for COATING 1,  $0.32\%$  for COATING 3,  $-0.23\%$  for COATING 2 and  $-0.10\%$  for untreated sample. After freeze–thaw cycles (EN 12371),  $\Delta V_p\% = -3$  and  $-4$  were determined for untreated and treated samples, respectively. The variation in elastic modulus  $\Delta E\%$  was  $-9$  on samples treated with COATING 1. The other coated samples provided  $\Delta E\% = -1$ .

Furthermore, Blue limestone is the stone where, considering  $\Delta V_p$  and  $\Delta E$ , no negative effect of applying hydrophobics coating can be interpreted, as the stone is relatively homogeneous and compact.

### 3.1.5. Destructive Tests: Flexural Strength

Flexural strength ( $\sigma_f$ ), to be assessed according to standard EN 12372, is a parameter commonly used for the design and dimensioning of wall claddings. After durability tests of natural stones, it is also required to evaluate the effects of weathering resulting from extreme temperature fluctuations in the presence of water, as specified by EN 14066 (thermal shock) and those resulting from cold temperature EN 12371 (freeze–thaw). In Table 12, values of  $\sigma_f$  (MPa) before and after tests are compared to quantify the variation in mechanical strength  $\Delta\sigma_f$  (%).

**Table 12.** Value of flexural strength  $\sigma_f$  (MPa) and its difference  $\Delta\sigma_f$  (%) before and after modified EN 14066 and EN 12372. COATING 1 = aminopropyltriethoxysilane; COATING 2 = aminefluorosilane; COATING 3 = methylmethoxysilane-based formulation.

Sample		$\sigma_f$ After EN 14066 (MPa)	$\sigma_f$ Pre-Test (MPa) and $\Delta\sigma_f$ (%) After EN 14066	$\sigma_f$ After EN 12371 (MPa)	$\sigma_f$ Pre-Test (MPa) and $\Delta\sigma_f$ (%) After EN 12371
Branco Untreated	average st. dev	6.5 $\pm 0.8$		7.7 $\pm 0.4$	
Branco COATING 1	average st. dev	7 $\pm 0.94$	8.27 $\pm 0.4$	5 $\pm 2.9$	8.27 $\pm 0.4$
Branco COATING 2	average st. dev	7.26 $\pm 0.43$	−13	1.72 $\pm 0.36$	−52
Branco COATING 3	average st. dev	8.12 $\pm 1$		1.46 $\pm 1.33$	
Lioz Untreated	average st. dev	12.88 $\pm 0.77$		11.3 $\pm 1.82$	
Lioz COATING 1	average st. dev	12.88 $\pm 2.12$	11.6 $\pm 0.9$	12.38 $\pm 0.31$	11.6 $\pm 0.9$
Lioz COATING 2	average st. dev	12.6 $\pm 3.82$	11	10.7 $\pm 1.25$	−1.6
Lioz COATING 3	average st. dev	13.57 $\pm 2.02$		11.24 $\pm 1.3$	
Alpinina Untreated	average st. dev	7.52 $\pm 1.89$		5.73 $\pm 0.12$	
Alpinina COATING 1	average st. dev	9.22 $\pm 1.40$	10.5 $\pm 2.8$	4.54 $\pm 3$	10.5 $\pm 2.8$
Alpinina COATING 2	average st. dev	7.23 $\pm 4$	−26	4.2 $\pm 1.32$	−53
Alpinina COATING 3	average st. dev	7.35 $\pm 3.12$		5.08 $\pm 0.72$	

**Table 12.** *Cont.*

Sample		$\sigma_f$ After EN 14066 (MPa)	$\sigma_f$ Pre-Test (MPa) and $D\sigma_f$ (%) After EN 14066	$\sigma_f$ After EN 12371 (MPa)	$\sigma_f$ Pre-Test (MPa) and $D\sigma_f$ (%) After EN 12371
Blue l. Untreated	average	9.85		11.37	
	st. dev	$\pm 2.84$		$\pm 4.32$	
Blue l. COATING 1	average	9.1		14.31	
	st. dev	$\pm 3.68$	15 $\pm$ 6.9	$\pm 4.38$	15 $\pm$ 6.9
Blue l. COATING 2	average	10.1		10.76	
	st. dev	$\pm 1.96$	-28	$\pm 4.7$	-22
Blue l. COATING 3	average	14.27		12.42	
	st. dev	$\pm 1.37$		$\pm 4.34$	

### Branco Results

In general, greater negative variation was achieved after performing EN 12371, in accordance with the damage suffered by the cyclic crystallization pressure of the ice. The variation in flexural strength  $\Delta\sigma_f$  after EN 14006 was equal to  $-13\%$ . After EN 12371, it was equal to  $-52\%$ . The lower values were detected on samples protected with hydrophobic coatings, which was in line with the determination of open porosity, ultrasound speed propagation, and elastic modulus.

When exposed to repeated freeze–thaw cycles, as specified by the EN 12371 standard, stones experience microcracking and disaggregation, facilitating water absorption. Hydrophobic coatings permeate the porous inner framework, probably altering the regular release of water absorbed through microcracks or fractures during the thawing process. Consequently, over successive freeze–thaw cycles, a larger amount of water is subjected to freezing, expanding ice within the porous framework. This expansion yields a generalized internal crystallization pressure, ultimately resulting in more significant damage than untreated stones.

Branco treated with COATING 1 (aminopropyltriethoxysilane) better performed with respect to COATING 2 (aminefluorosilane) and COATING 3 (methylmethoxysilane-based formulation). Even COATING 3 gave a higher result after EN 14066. COATING 2 can be considered a good formulation in terms of the maintenance of hydrophobicity. The static contact angle was in the following range:  $87^\circ < \Theta^\circ < 100^\circ$  after EN 14066 and  $100^\circ < \Theta^\circ < 124^\circ$  after EN 12371 (Table 8).

### Lioz Results

Lioz is strongly heterogeneous because of stylolites with different amount and openings. So, since the flexural strength test is destructive, comparisons values before and after cannot be properly conducted as the specimens are naturally different, and each sample differs significantly from the other. Effectively, after thermal shock (EN 14066), the variation is positive ( $\Delta\sigma_f = 11\%$ ), and after freeze–thaw (EN 12371), it is just  $\Delta\sigma_f = -1.6\%$ . Thus, all coated samples have satisfactory flexural strength. They are also the samples with higher hydrophobicity after thermal-shock and freeze–thaw cycles (Table 8).

### Alpinina Results

Although the stone is very compact and resistant, it suffered a  $\Delta\sigma_f = -26\%$  after thermal-shock cycles and  $\Delta\sigma_f = -53\%$  after freeze–thaw cycles. The presence of sparite in Lioz A and Alpinina limestones could suggest a higher susceptibility to decay, as found in Alpinina and other sparite-rich limestone [53,54]. This can explain this unexpectedly high  $\Delta\sigma_f$  (%), mostly after freeze–thaw (EN 12371), as well as the difference in open porosity, ultrasound velocity, and elastic modulus. There seems to be no correlation between the values of  $\sigma_f$  and degree of wettability and static contact angle ( $85^\circ < \Theta^\circ < 115^\circ$  after EN 14066 and  $55^\circ < \Theta^\circ < 136^\circ$  after EN 12371, Table 8). Still, for sure, all coatings suffered from thermal-shock cycles and less from freeze–thaw cycles, except COATING 1, which lost its initial efficacy ( $55^\circ < \Theta^\circ < 61^\circ$ ).

### Blue Limestone Results

Regarding this stone, after thermal shock (EN 14066), values highlight a  $\Delta\sigma_f = -28\%$ , and after freeze–thaw (EN 12371),  $\Delta\sigma_f = -22\%$ . The small heterogeneities of blue limestone influence the correlation between pre- and post-test.  $\Delta\sigma_f$  is in accordance with the entity of damage detected with the elastic modulus, which is higher after EN 12371 but in contrast to the value of increased open porosity (up to 53%). In general, the static contact angle, except COATING 1 samples, revealed better resistance to freeze–thaw. COATING 2 confers good protection in environments with high thermal variation and cold temperatures and offers high hydrophobicity. The static contact angle  $\Theta^\circ$  is in the interval between  $99^\circ$  and  $112^\circ$  after EN 14066 and  $97^\circ < \Theta^\circ < 119^\circ$  after EN 12371.

## 4. Discussions

The long-term performance of different Portuguese limestones subjected to heating–cooling cycles (thermal shock) and freeze–thaw aging is foreseen, and the efficiency of three commercial hydrophobic coatings (aminopropyltriethoxysilane; aminefluorosilane; methylmethoxysilane-based formulation) is assessed. The European Standards EN 14066:2013 for determining resistance to aging by thermal shock and EN 12371:2010 for assessing frost resistance were followed.

The multi-analytical approach, considering the mass and porosity variation and the determination of wettability of stones through the measure of static contact angle, yielded promising results in terms of water protection capabilities of the coatings during aging. The evaluation of sound speed propagation, associated with the quality of building material, measurement of elastic modulus and flexural strength disclosed the alteration, structural integrity, and mechanical resistance of the stones.

The coatings exhibited an overall good preservation of hydrophobicity even after undergoing abrupt thermal-shock and freeze–thaw tests. The coatings demonstrate a deleterious influence on the structural integrity of stones, especially porous limestones like Branco. This study reveals a critical interaction between freeze–thaw cycles, hydrophobic coatings, and stone. Untreated porous stones maintain their structural integrity effectively, enabling them to release water naturally during freeze–thaw cycles. Conversely, in the case of treated samples, when natural microcracks form and water is absorbed, the use of hydrophobic coatings might clog pores and hinder water release due to the partial sealing of the porous structure, potentially leading to severe fractures and mechanical damage to the stone during the following cycle of freezing. Over successive freeze–thaw cycles, this process intensifies the internal crystallization pressure of the ice within the stone, resulting in severe pathologies. Thus, it is evident that “protective” coatings, intended to safeguard the stone structures in the presence of water, could contribute to their deterioration under such climatic conditions. This phenomenon is more evident in more porous limestones, but authors cannot exclude that structural damage may occur over a longer period, even in more compact and homogeneous stones. Alpinina revealed an unexpected behavior, manifesting a noticeable reduction in its physical and mechanical properties. Lioz and Blue limestone are more compact heterogeneous stones. The inherent variability among

specimens is crucial, and caution is recommended when making direct comparisons before and after testing.

Considering this, the difficulty in choosing a single suitable product and the importance of a comprehensive understanding of the decay mechanisms in the preservation of stone, with implications for material conservation in the long term, must be underlined.

These outcomes contribute to our understanding of stone durability and the efficacy of silane/siloxane based hydrophobic protective measures, providing important insights for a sustainable design, preservation and maintenance of stone materials in construction and architectural applications.

## 5. Conclusions

The findings of this study offer a perspective on the complex interaction between silane-siloxane-based hydrophobic coatings and the durability of natural stones under durability laboratory tests, freeze-thaw and thermal-shock aging. While the coatings demonstrated general satisfactory effectiveness in maintaining hydrophobicity, their role in the overall preservation of porous limestones presents challenges that warrant careful consideration. The ability of untreated stones to naturally absorb and release water during freeze-thaw cycles emerged as a significant factor in maintaining structural integrity. Conversely, the application of hydrophobic treatments, intended to shield the material from water damage, sometimes impeded this natural process, leading to internal pressures that exacerbated microcracking and structural degradation.

This paradox reveals a crucial need to adapt preservation strategies to the intrinsic properties of different stone types. The findings highlight that the protective measures applied must be tailored to not only safeguard against immediate threats but also to accommodate the long-term mechanical behaviors of these materials. Stones with higher porosity proved particularly vulnerable to the unintended consequences of hydrophobic treatments, while more compact stones exhibited greater resilience.

The implications of this study extend beyond technical assessments, prompting a re-thinking of conservation practices in the face of climate-induced environmental challenges. With temperature fluctuations and moisture pattern alterations, the strategies employed to preserve ancient and contemporary architectural heritage must evolve. A more holistic approach that integrates advanced material diagnostics and context-specific applications is essential. Future research should focus on developing innovative formulations and methods that mitigate the identified drawbacks while enhancing the protective benefits of coatings.

**Author Contributions:** C.L.: Project administration, Funding acquisition, Conceptualization, Methodology, Data curation, Formal analysis, Investigation, Resources, Software, Validation, Visualization, Writing—original draft, Writing—review and editing. F.S.: Validation, Visualization, Review and editing. V.P.: Visualization, Validation, Writing—review and editing. J.M.: Supervision, Funding acquisition, Validation, Visualization, Writing—review and editing. All authors have read and agreed to the published version of the manuscript.

**Funding:** Carla Lisci gratefully acknowledges FCT for the grant SFRH/BD/149699/2019 co-funded by the European Social Fund (ESF) and MEC national funds. Carla Lisci gratefully acknowledges Roberto Madorno for the constant technical and scientific support on the chemistry and the application of the protective treatments. Fabio Sitzia gratefully acknowledges the Recursos Humanos Altamente Qualificados for the contract with Ref. ALT2059-2019-24. Vera Pires gratefully acknowledges the Contrato Programa entre FCT e a Universidade de Évora no âmbito do concurso estímulo ao emprego científico institucional 2018. The authors gratefully acknowledge the following funding sources: INOVSTONE4.0 (POCI-01-0247-FEDER-024535), co-financed by the European Union through the European Regional Development Fund (FEDER) and Fundação para a Ciência e Tecnologia (FCT) under the project UID/Multi/04449/2013 (POCI-01-0145-FEDER-007649), and Fundacão para a Ciencia e Tecnologia (FCT) under the project UIDB/04449/2020 and UIDP/04449/2020. The authors gratefully acknowledge the European Communion—Portugal, Grant Contract number: Sustainable Stone by

Portugal, Call: 2021-C05i0101-02—agendas/alianças mobilizadoras para a reindustrialização—PRR, Proposal: C632482988-00467016.

**Data Availability Statement:** Data is contained within the article.

**Conflicts of Interest:** The authors declare no conflict of interest.

## References

1. Siegesmund, S.; Snethlage, R. *Stone in Architecture: Properties, Durability: Fifth Edition*; Springer: Berlin/Heidelberg, Germany, 2014; ISBN 9783642451553.
2. Lisci, C.; Sitzia, F. *Degrado, Danni e Difetti Delle Pietre Naturali e Dei Laterizi. Meccanismi Di Alterazione, Patologie, Tecniche Diagnostiche e Schede Pratiche*; Maggioli: Sant’Arcangelo di Romagna, Italy, 2021; ISBN 8891650351.
3. Aldred, J.; Eppes, M.C.; Aquino, K.; Deal, R.; Garbini, J.; Swami, S.; Tuttle, A.; Xanthos, G. The Influence of Solar-Induced Thermal Stresses on the Mechanical Weathering of Rocks in Humid Mid-Latitudes. *Earth Surf. Process. Landf.* **2016**, *41*, 603–614. [[CrossRef](#)]
4. Erguler, Z.A.; Shakoor, A. Relative Contribution of Various Climatic Processes in Disintegration of Clay-Bearing Rocks. *Eng. Geol.* **2009**, *108*, 36–42. [[CrossRef](#)]
5. Gómez-Heras, M.; Smith, B.J.; Fort, R. Surface Temperature Differences between Minerals in Crystalline Rocks: Implications for Granular Disaggregation of Granites through Thermal Fatigue. *Geomorphology* **2006**, *78*, 236–249. [[CrossRef](#)]
6. Kelly, W.C.; Zumberge, J.H. Weathering of a Quartz Diorite at Marble Point, McMurdo Sound, Antarctica. *J. Geol.* **1961**, *69*, 433–446. [[CrossRef](#)]
7. Peel, R.F. *Zeitschrift für Geomorphologie*; Gebruder Borntraeger: Stuttgart, Germany, 1974; pp. 19–28.
8. Pires, V.; Rosa, L.G.; Dionísio, A. Implications of Exposure to High Temperatures for Stone Cladding Requirements of Three Portuguese Granites Regarding the Use of Dowel-Hole Anchoring Systems. *Constr. Build. Mater.* **2014**, *64*, 440–450. [[CrossRef](#)]
9. Dionísio, A. Stone Decay Induced by Fire on Historic Buildings: The Case of the Cloister of Lisbon Cathedral (Portugal). *Geol. Soc. Spec. Publ.* **2007**, *271*, 87–98. [[CrossRef](#)]
10. McGreevy, J.P.; Warke, P.A.; Smith, B.J. Controls on Stone Temperatures and the Benefits of Interdisciplinary Exchange. *J. Am. Inst. Conserv.* **2000**, *39*, 259. [[CrossRef](#)]
11. Jenkins, K.A.; Smith, B.J. Daytime Rock Surface Temperature Variability and Its Implications for Mechanical Rock Weathering: Tenerife, Canary Islands. *Catena* **1990**, *17*, 449–459. [[CrossRef](#)]
12. Hall, K.; André, M.F. Rock Thermal Data at the Grain Scale: Applicability to Granular Disintegration in Cold Environments. *Earth Surf. Process. Landf.* **2003**, *28*, 823–836. [[CrossRef](#)]
13. Yang, W.H.; Srolovitz, D.J.; Hassold, G.N.; Anderson, M. The Effect of Grain Boundary Cohesion on the Fracture of Brittle, Polycrystalline Materials. In *Simulation and Theory of Evolving Microstructures*; Anderson, M.P., Rollett, A.D., Eds.; The Metallurgical Society: Warrendale, PA, USA, 1990; ISBN 978-0873391184.
14. Siegesmund, S.; Ruedrich, J.; Koch, A. Marble Bowing: Comparative Studies of Three Different Public Building Facades. *Environ. Geol.* **2008**, *56*, 473–494. [[CrossRef](#)]
15. Vázquez, P.; Siegesmund, S.; Alonso, F.J. Bowing of Dimensional Granitic Stones. *Environ. Earth Sci.* **2011**, *63*, 1603–1612. [[CrossRef](#)]
16. Sitzia, F.; Lisci, C.; Pires, V.; Alves, T. Laboratorial Simulation for Assessing the Performance of Slates as Construction Materials in Cold Climates. *Appl. Sci.* **2023**, *13*, 2761. [[CrossRef](#)]
17. Deprez, M.; De Kock, T.; De Schutter, G.; Cnudde, V. A Review on Freeze-Thaw Action and Weathering of Rocks. *Earth-Science Rev.* **2020**, *203*, 103143. [[CrossRef](#)]
18. Ruedrich, J.; Kirchner, D.; Siegesmund, S. Physical Weathering of Building Stones Induced by Freeze–Thaw Action: A Laboratory Long-Term Study. *Environ. Earth Sci.* **2011**, *63*, 1573–1586. [[CrossRef](#)]
19. Snethlage, R. *Steinkonservierung*; Bayerisches Landesamt Fur Denkmalpflege: Munich, Germany, 1982.
20. Fitzner, B.; Snethlage, R. *Einfluß Der Porenradienverteilung Auf Das Verwitterungsverhalten Ausgewählter Sandsteine*; Bautenschu: Birmingham, UK, 1982.
21. Weiss, G. *Die Eis Und Salzkristallisation Im Porenraum von Sandsteinen Und Ihre Auswirkung Auf Das Gefüge Unter Besonderer Berücksichtigung Gesteinsspezifischer Parameter*; Münchner: Munich, Germany, 1992.
22. Power, T. A Working Hypothesis for Further Studies of Frost Resistance of Concrete. *ACI J. Proc.* **1945**, *41*, 245–272. [[CrossRef](#)]
23. Merriam, R.; Rieke, H.H.; Kim, Y.C. Tensile Strength Related to Mineralogy and Texture of Some Granitic Rocks. *Eng. Geol.* **1970**, *4*, 155–160. [[CrossRef](#)]
24. Ghobadi, M.H.; Babazadeh, R. Experimental Studies on the Effects of Cyclic Freezing–Thawing, Salt Crystallization, and Thermal Shock on the Physical and Mechanical Characteristics of Selected Sandstones. *Rock Mech. Rock Eng.* **2015**, *48*, 1001–1016. [[CrossRef](#)]
25. Sousa, H.; Sousa, R. Durability of Stone Cladding in Buildings: A Case Study of Marble Slabs Affected by Bowing. *Buildings* **2019**, *9*, 299. [[CrossRef](#)]
26. Hamzaban, M.-T.; Büyüksaçış, I.S.; Touranchehzadeh, A.; Manafi, M. The Effect of Heat Shocks and Freezing–Thawing Cycles on the Mechanical Properties of Natural Building Stones. *J. Mod. Mech. Eng. Technol.* **2021**, *8*, 76–100. [[CrossRef](#)]

27. Al-Omari, A.; Beck, K.; Brunetaud, X.; Török, Á.; Al-Mukhtar, M. Critical Degree of Saturation: A Control Factor of Freeze-Thaw Damage of Porous Limestones at Castle of Chambord, France. *Eng. Geol.* **2015**, *185*, 71–80. [[CrossRef](#)]
28. Everett, D.H. The Thermodynamics of Frost Damage to Porous Solids. *Trans. Faraday Soc.* **1961**, *57*, 1541–1551. [[CrossRef](#)]
29. EN 14066:2013; Natural Stone Test Methods—Determination of Resistance to Ageing by Thermal Shock. European Committee for Standardization (CEN): Brussels, Belgium, 2013. Available online: <https://store.uni.com/en/uni-en-14066-2013> (accessed on 17 November 2024).
30. EN 12371:2010; Natural Stone Test Methods—Determination of Frost Resistance (in Portuguese). European Committee for Standardization (CEN): Brussels, Belgium, 2010. Available online: <https://store.uni.com/en/en-12371-2010> (accessed on 17 November 2024).
31. Folk, R.L. Practical Petrographic Classification of Limestones. *Am. Assoc. Pet. Geol. Bull.* **1959**, *43*, 1–38.
32. EN 16581:2014; Conservation of Cultural Heritage—Surface Protection for Porous Inorganic Materials—Laboratory Test Methods for the Evaluation of the Performance of Water Repellent Products. European Committee for Standardization (CEN): Brussels, Belgium, 2014. Available online: <https://store.uni.com/en/en-16581-2014> (accessed on 17 November 2024).
33. Darmawan, A.; Utari, R.; Saputra, R.E.; Suhartana; Astuti, Y. Synthesis and Characterization of Hydrophobic Silica Thin Layer Derived from Methyltrimethoxysilane (MTMS). *IOP Conf. Series Mater. Sci. Eng.* **2018**, *299*, 012041. [[CrossRef](#)]
34. Laskowski, L.; Laskowska, M.; Jelonkiewicz, J.; Dulski, M.; Wojtyniak, M.; Fitta, M.; Balandz, M. SBA-15 Mesoporous Silica Free-Standing Thin Films Containing Copper Ions Bounded via Propyl Phosphonate Units—Preparation and Characterization. *J. Solid State Chem.* **2016**, *241*, 143–151. [[CrossRef](#)]
35. Wicks, Z.W.; Jones, F.N.; Pappas, S.P.; Wicks, D.A. *Organic Coatings: Science and Technology*; Wiley Edition: Hoboken, NJ, USA, 2006; ISBN 9780471698067.
36. Witucki, G.L. Silane Primer: Chemistry and Applications of Alkoxy Silanes. *J. Coatings Technol.* **1993**, *65*, 57–60.
37. Lisci, C.; Pires, V.; Sitzia, F.; Mirão, J. Limestones Durability Study on Salt Crystallisation: An Integrated Approach. *Case Stud. Constr. Mater.* **2022**, *17*, e01572. [[CrossRef](#)]
38. Germinario, L.; Andriani, G.F.; Laviano, R. Decay of Calcareous Building Stone under the Combined Action of Thermoclastism and Cryoclastism: A Laboratory Simulation. *Constr. Build. Mater.* **2015**, *75*, 385–394. [[CrossRef](#)]
39. Ugur, I. Surface Characterization of Some Porous Natural Stones Modified with a Waterborne Fluorinated Polysiloxane Agent under Physical Weathering Conditions. *J. Coatings Technol. Res.* **2014**, *11*, 639–649. [[CrossRef](#)]
40. Striani, R.; Corcione, C.E.; Anna, G.D.; Frigione, M. Progress in Organic Coatings Durability of a Sunlight-Curable Organic–Inorganic Hybrid Protective Coating for Porous Stones in Natural and Artificial Weathering Conditions. *Prog. Org. Coatings* **2016**, *101*, 1–14. [[CrossRef](#)]
41. Durmeková, T.; Adamcová, R.; Maľa, M.; Grand, P. Efficiency of Protective Coating Applied on a Highly Porous Decorative Tuff. *Acta Geol. Slovaca* **2021**, *13*, 85–94.
42. EN 1936:2006; Natural Stone Test Method. Determination of Real Density and Apparent Density, and of Total and Open Porosity 3. European Committee for Standardization (CEN): Brussels, Belgium, 2006. Available online: <https://store.uni.com/en/en-1936-2006> (accessed on 17 November 2024).
43. EN 14579:2004; Natural Stone Test Methods—Determination of Sound Speed Propagation. European Committee for Standardization (CEN): Brussels, Belgium, 2007. Available online: <https://store.uni.com/en/en-14579-2004> (accessed on 17 November 2024).
44. Kahraman, S.; Ulker, U.; Delibalta, M.S. A Quality Classification of Building Stones from P-Wave Velocity and Its Application to Stone Cutting with Gang Saws. *J. South. African Inst. Min. Metall.* **2007**, *107*, 427–430. [[CrossRef](#)]
45. Fais, S.; Cuccuru, F.; Ligas, P.; Casula, G.; Bianchi, M.G. Integrated Ultrasonic, Laser Scanning and Petrographical Characterisation of Carbonate Building Materials on an Architectural Structure of a Historic Building. *Bull. Eng. Geol. Environ.* **2015**, *76*, 71–84. [[CrossRef](#)]
46. Cuccuru, F.; Fais, S.; Ligas, P. Dynamic Elastic Characterization of Carbonate Rocks Used as Building Materials in the Historical City Centre of Cagliari (Italy). *Q. J. Eng. Hydrogeol.* **2014**, *47*, 259–266. [[CrossRef](#)]
47. EN 14146:2004; Determination of Dynamic Modulus of Elasticity (by Measuring the Fundamental Resonance Frequency). European Committee for Standardization (CEN): Brussels, Belgium, 2004. Available online: <https://store.uni.com/en/en-14146-2004> (accessed on 17 November 2024).
48. EN 12372:2022; Natural Stone Test Methods—Determination of Flexural Strength under Concentrated Load. The British Standards Institution: London, UK, 2003. Available online: <https://store.uni.com/en/en-12372-2022> (accessed on 17 November 2024).
49. EN 16140:2019; Determination of Sensitivity to Changes in Appearance Produced by Thermal Cycles. European Committee for Standardization (CEN): Brussels, Belgium, 2013. Available online: <https://store.uni.com/en/en-16140-2019> (accessed on 17 November 2024).
50. Young, T. An Essay on the Cohesion of Fluids. *Philosophical Transactions of the Royal Society of London* **1805**, *95*, 65–87. [[CrossRef](#)]
51. Favaro, M.; Mendichi, R.; Ossola, F.; Russo, U.; Simon, S.; Tomasin, P.; Vigato, P.A. Evaluation of Polymers for Conservation Treatments of Outdoor Exposed Stone Monuments. Part I: Photo-Oxidative Weathering. *Polym. Degrad. Stab.* **2006**, *91*, 3083–3096. [[CrossRef](#)]
52. Clegg, C. Contact Angle Made Easy. Carl Clegg, 2013; ISBN 9781300662983.

53. Sousa, L.; Menningen, J.; López-Doncel, R.; Siegesmund, S. Petrophysical Properties of Limestones: Influence on Behaviour under Different Environmental Conditions and Applications. *Environ. Earth Sci.* **2021**, *80*, 1–19. [[CrossRef](#)]
54. Akram, M.S.; Farooq, S.; Naeem, M.; Ghazi, S. Prediction of Mechanical Behaviour from Mineralogical Composition of Sakesar Limestone, Central Salt Range, Pakistan. *Bull. Eng. Geol. Environ.* **2017**, *76*, 601–615. [[CrossRef](#)]

**Disclaimer/Publisher’s Note:** The statements, opinions and data contained in all publications are solely those of the individual author(s) and contributor(s) and not of MDPI and/or the editor(s). MDPI and/or the editor(s) disclaim responsibility for any injury to people or property resulting from any ideas, methods, instructions or products referred to in the content.